Capsim Application Note

9600 bps Full-Duplex Voice Band Data Communicatio.

With Adaptive Equalization and Echo Cancellation

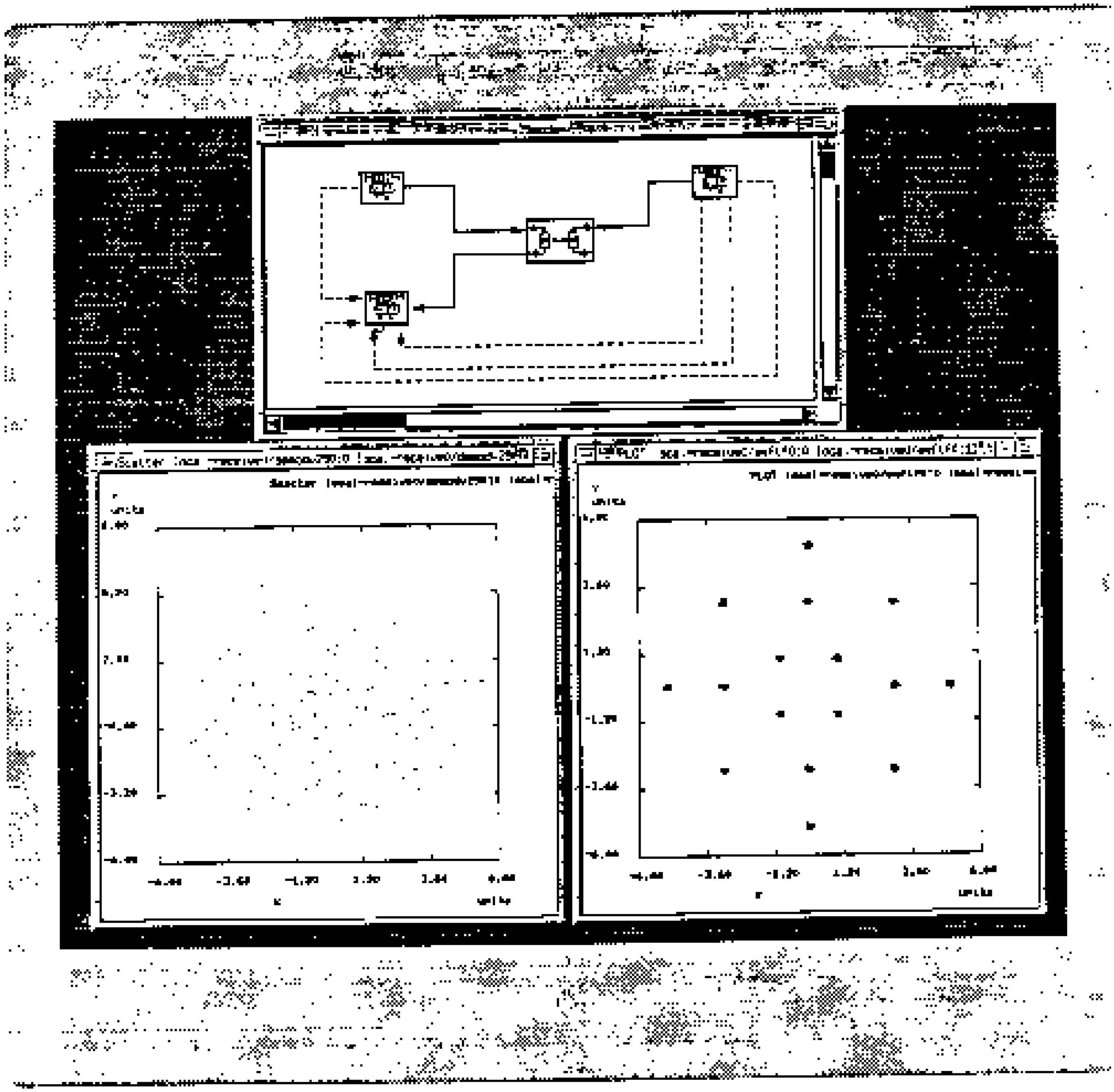

Design by Ali Soheil Sadri and Tulay Adali

This work was supported by Datec Inc.
Research Triangle Park, NC Under
National Science Foundation SBIR Grant Number ISI-8960842. (October 1990)

1. Introduction

The word "modem" is a concatenation of MODulator and DEModulator, but there is a wide range of opinion as to what constitutes modulation and demodulation, and whether, a modem should comprise more than just a *mod* and a *dem*. The traditional definition of a *mod* is " a device that accepts serial binary pulses from a data source and modulates some property (amplitude, frequency, or phase) of an analog signal in order to create a signal suitable for transmission in an analog medium." [29] The following example illustrates the design and simulation of a 9600 bps V.29 modem with adaptive equalization and echo cancellation using the Capsim simulation package. In the first part of this report we will discuss the modem design in a hierarchical fashion. We start with a top level topology and then move down into small blocks and describe them separately. In Capsim glossary, the name *Star* refers to a indivisible block in the simulation and the name *Galaxy* refers to combination of several connected blocks. These blocks can be either stars or galaxies! The second part of this report presents a performance comparison between the two known adaptive filtering algorithms, the LMS algorithm and the general order multichannel fast transversal filter algorithm [32], for both echo cancellation and equalization. The Fast Transversal Filter [2] is an efficient implementation of the Recursive Least Squares algorithm. In [4],[5] and ,[32], this algorithm was generalized to multiple input and multiple output systems with arbitrary orders. The adaptive filters in high speed modems are generally of this type. For example, the fractionally spaced equilizer with decision feedback, or a pole-zero type echo canceller. A fixed point implementation of the echo canceller will also be presented and its effects on the bit error rate and signal contellation will be shown.

This application note is very brief and only touches on some topics. The idea is to show how a complex system may be simulated using Capsim, and also introduce the power of advanced adaptive filtering algorithms. The reader interested in more detail is refered to the references. For a discussion on the RLS algorithm and its applications to telecommunications refer to references [1-6] and [33-34]. For an analysis of finite precision issues see references [7-19], in particular for an overview see [12]. A good reference on equalization is [33]. Finally, an excelent paper, which provides a historical perspective to the various advances that have made high speed digital communication possible, is [35].

2. Modem Design

The principle characteristics of the CCITT V.29 recommendations for transmitting data at 9600 bps are as follows [28]:

a) capable of operating in a four wire duplex or half duplex mode with continuous or controlled carrier;
b) combined amplitude and phase modulation;
c) inclusion of an automatic adaptive equalizer.

The top level block diagram of the system is shown in Fig. 1. This system consists of a remote transmitter, a telephone channel with hybrids, a local transmitter and finally a local receiver. Each of these blocks will be described in detail later in this report.

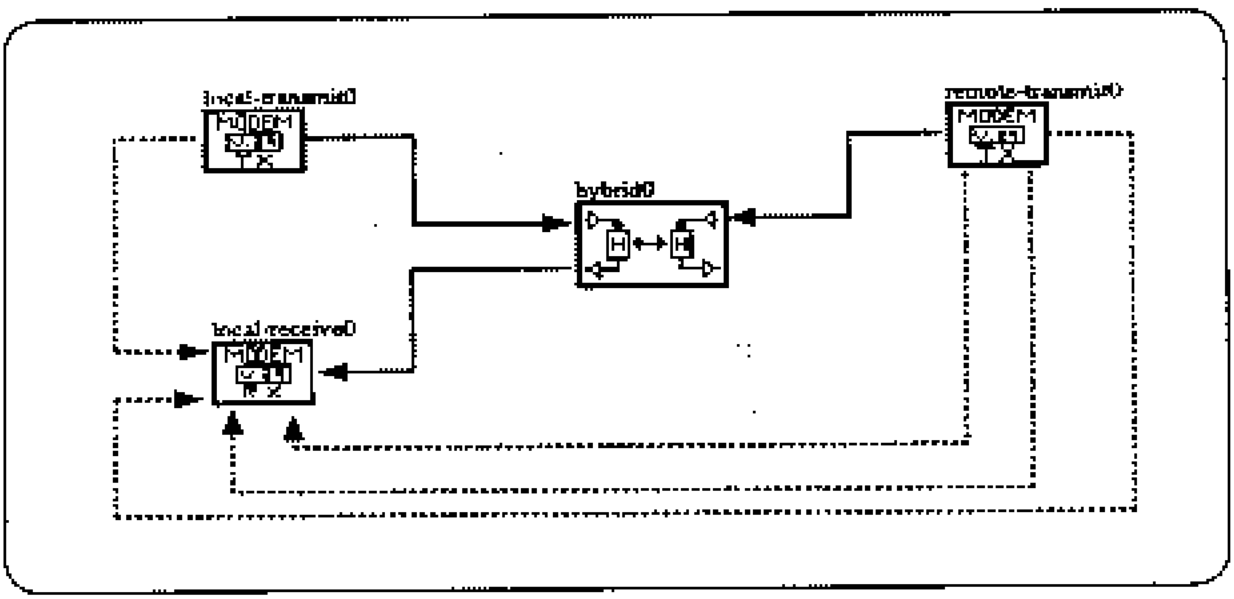

Figure 1. Top level block diagram

The task of the V.29 encoder is to output one symbol for every four bits. Thus, if the bit rate is 9600 bps, the symbol rate is 2400 symbols/sec. The symbols are complex numbers which correspond to the coordinates of the signal constellations. Fig. 2 shows the sixteen point constellation of the CCITT V.29 recommendations.

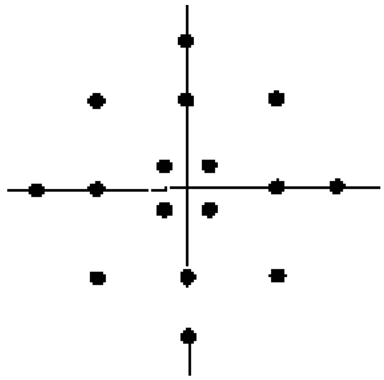

Figure 2. Signal space diagram at 9600 bps

At 9600 bits per second, the scrambled data stream to be transmitted is divided into groups of four consecutive data bits (quad bits). The first bit (Q1) of each quad bit is used to determine the signal element amplitude to be transmitted. The second (Q2), third (Q3), and the fourth (Q4) bits are encoded as phase change relative to the phase of the immediately preceding element. This phase encoding is identical to recommendations V.27 [28].

3. System Description

3.1. Remote transmitter

As mentioned before, this system is divided into several galaxies. In a full duplex voice band modem the remote transmitter encodes the data bits, modulates them, and transmits the signal into the channel. Fig. 3 illustrates the galaxy remote-transmit in detail.

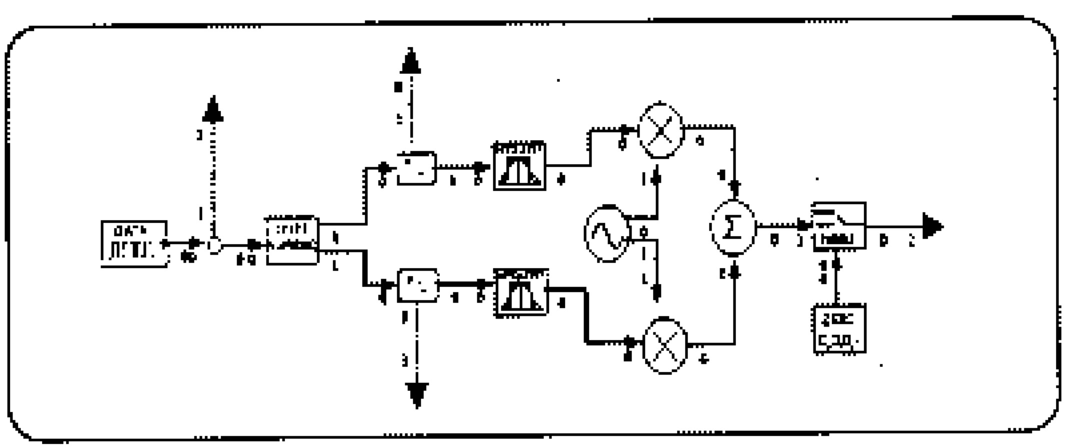

Figure 3. Block diagram of the encoder and the transmitter

The first star in this galaxy is the binary data generator (*bdata*). Since this data is random, for simplicity no scrambler is used in this simulation. In our case, 16384 data bits are produced by this block. This star is connected to the *v29encoder* star via a node. A *node* (shown as a small circle) is used in order to send the same data bits into the *ecount* star for error counting. The *v29encoder* star produces the V.29 constellation coordinates. Buffer(0) carries the in-phase values and Buffer(1) carries the quadrature values. The output of this star produces a 2400 baud baseband signal. Each output of the encoder is over-sampled by 4 in order to produce a signal with a sampling rate of 9600 samples per second. This signal is passed through a square root Nyquist pulse shaping filter which is a raised cosine filter with a roll off factor of 20%. This action produces a baseband signal with a bandwidth of 1700 Hz. A complex modulation takes place after filtering. According to the CCITT V.29 recommendations, the carrier frequency of a 9600 bits per second modem is 1700 Hz [28]. Fig. 4 illustrates the spectrum of the baseband in-phase signal after passing through the Nyquist filter.

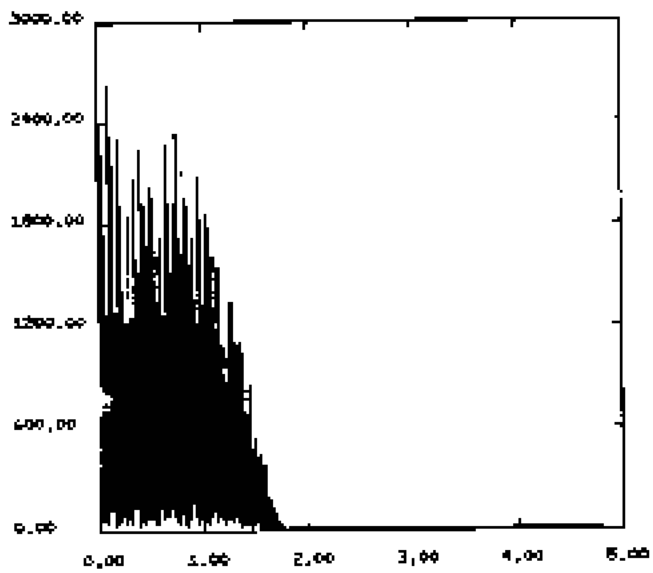

Figure 4. Signal after Nyquist filter (freq. KHz)

As we indicated previously, the 20% roll off factor in the Nyquist filter produces a lowpass filter with a band width of 1.7 KHz. Therefore, after modulation we obtain a passband signal with a band width of 3400 Hz. Fig. 5 illustrates the spectrum of the passband signal.

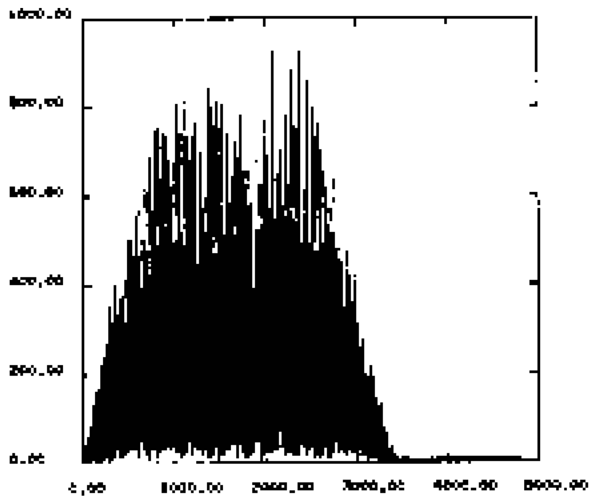

Figure 5. Complex signal after modulation (freq. Hz)

As is evident from Fig. 3, after the addition of the two in-phase and quadrature signals, the complex baseband signal passes through a *toggle* star. This star shuts off the remote transmitter during the local echo canceller adaptation process.

3.2. Local Transmitter

Fig. 6 illustrates the local-transmitter galaxy. The description of this galaxy is very similar to the remote-transmitter galaxy. The only difference is in the parameter of the *bdata* star; which is the value of the seed in the random generator and the absence of a *toggle* star.

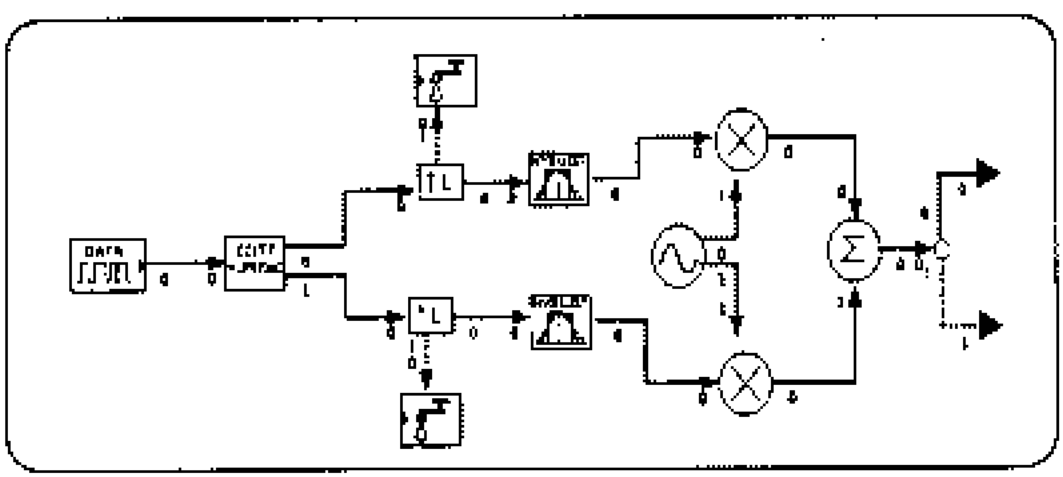

Figure 6. Block diagram of the local transmitter

3.3. Telephone Circuit Channel

One of the requirements in high speed data transmission is the ability to transmit signals in both directions (full-duplex transmission) on a single pair of wires. This is possible through the use of a four-wire to two-wire converter or "hybrid." If the balancing impedance within the hybrid is identical to the input impedance of the cable, the transmitted signal is completely isolated from the input to the receiver. However, a perfect match is difficult to achieve, especially over the 4 KHz bandwidth. Therefore, a "hybrid leakage" or "echo" represents a serious obstacle to full-duplex transmission . In this simulation, for simplicity, we have modeled the full-duplex voice band channel as a one directional channel. Fig. 7 illustrates this channel.

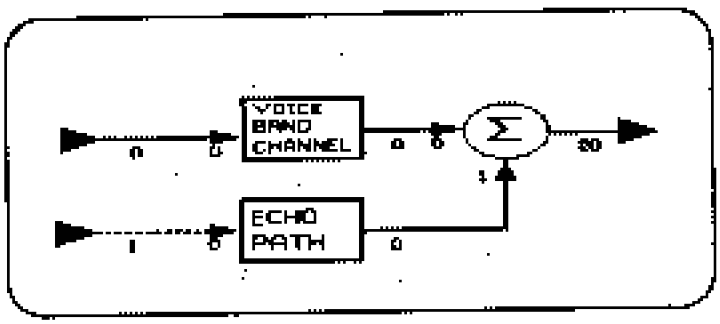

Figure 7. Model for the telephone circuit channel

The input terminal(0) of the above galaxy receives the signal from the remote transmitter and passes it through a voice band channel. The input terminal(1), on the other hand, receives the signal from the local transmitter and passes it through the *echopath* galaxy where the echo is produced. These two signals, the echo and the signal, add together and proceed toward the echo canceller. Fig. 8 illustrates the *echopath* galaxy.

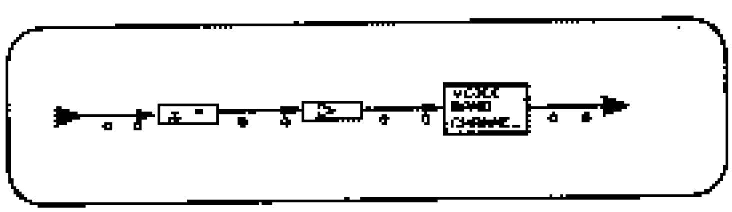

Figure 8. Echo path model

The echo is generated by delaying the local transmitter signal and passing it through a *gain* star which attenuates the signal. Both the echo and the signal are passed through the voice band channel. This voice band channel is modeled by an IIR filter with a bandwidth of roughly 4 KHz and an analog to digital converter with a μ-law compander. Fig. 9 illustrates the voiceband galaxy in detail.

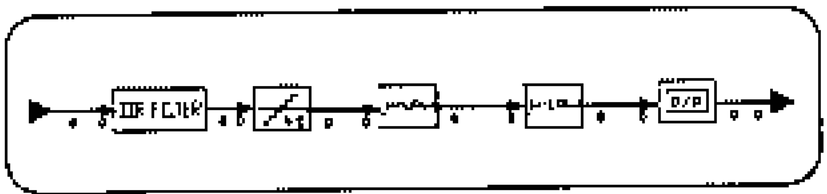

Figure 9. Model of the voice band channel

Fig. 10 illustrates the frequency response of the voice band channel.

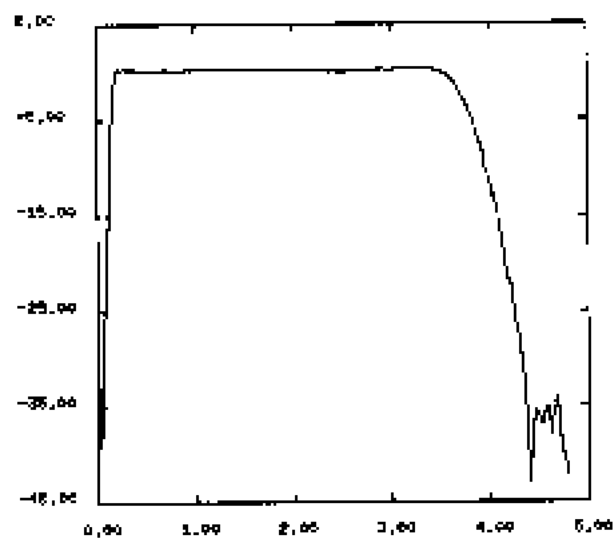
Figure 10. Frequency response of the voice band channel (freq. KHz)

The group delay response of the voice band channel implemented in this simulation is plotted in Fig. 11. This plot satisfies the limit of the CCITT M.1020 recommendations [28].

As shown from Fig. 9, the incoming signals are converted into digital signals and pass through the μ-law compressor and expander stars. Prior to leaving the voice band

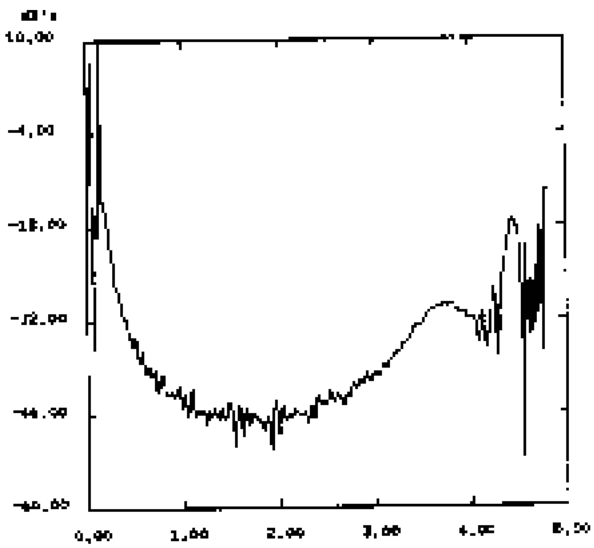

Figure 11. Group delay responce of the channel (freq. KHz)

channel, they are converted back into analog signals. These actions introduce quantization noise into the system. This noise which is caused by the non-uniform quantization scheme is a non-linear distortion which could cause a problem for the adaptive echo canceller [30].

3.4. Local Receiver

The last and the most complicated galaxy in this simulation is the local-receive galaxy. Multiple levels of the hierarchy are noticeable within this galaxy. Fig. 12 illustrates the block diagram of the local receiver.

3.4.1 Echo Canceller

The top left block in the local receiver galaxy is the echo canceller which is called *adapt-filter* galaxy. This is a 16 tap passband echo canceller which uses the fast RLS adaptive filtering algorithm [2,3,32]. The input terminal(0) of the echo canceller is the echo path of the adaptive filter and is connected to the output of the local-transmit galaxy. Input terminal(1) receives the signal with the echo from the output of the telephone circuit channel.

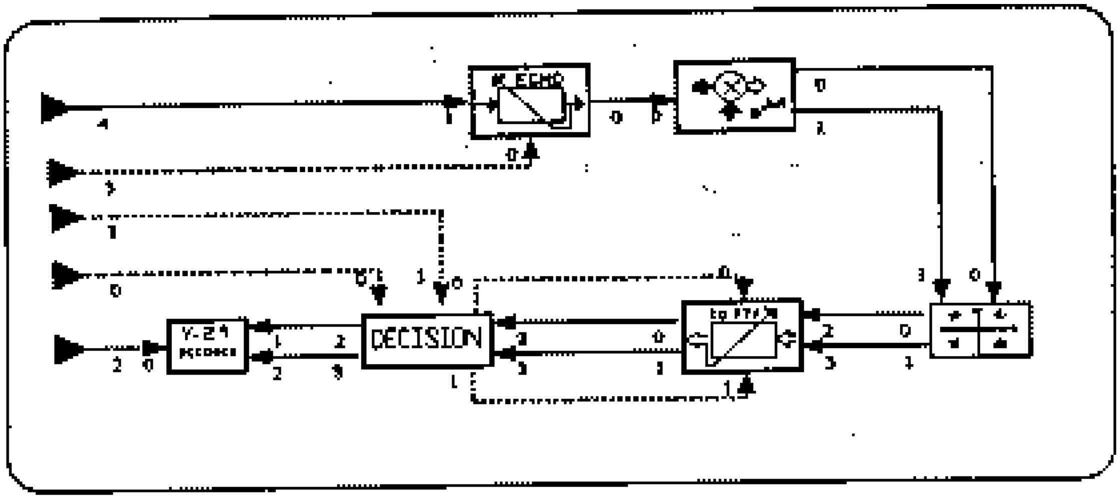

Figure 12. Block diagram of the local receiver

In this galaxy is the *predftf* star implements the multichannle general order fast RLS adaptive filtering algorithm of [3 ·]. This star can implement both the adaptive echo canceller and the equalizer. Fig. 13 illustrates the block diagram of the echo canceller. The predftf star uses the auto fan-in and auto fan-out facility in Capsim. Thus, it automatically adjusts itself to the various adaptive filtering configurations which require multiple inputs and outputs. A good example of a star with auto fan-in is the *add* star which can add two, three, or any number of input channels.

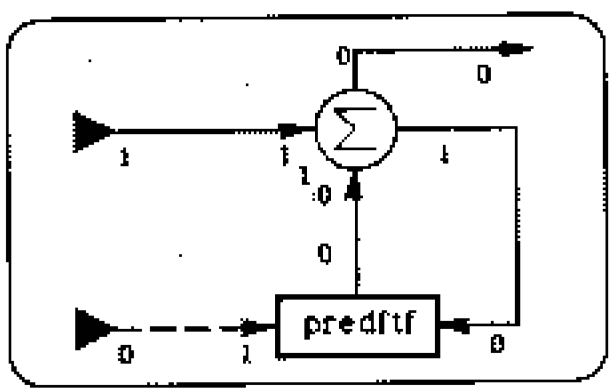

Figure 13. Block diagram of the passband echo canceller

3.4.2 Complex Demodulation

After echo cancellation, the signal enters a complex demodulation block. Fig. 14 illustrates the *demodv29* galaxy.

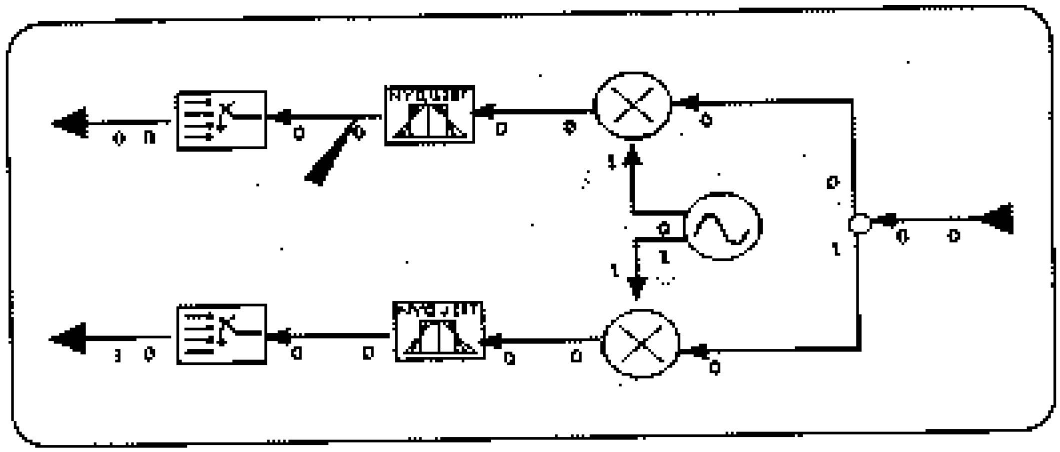

Figure 14. Block diagram of the complex demodulator

The incoming real signal splits into two in order to demodulate the in-phase and the quadrature components. The resulting passband signals are demodulated by mixing them with the 1700 Hz carrier. Lowpass matched filters are then employed to remove the double carrier component and to produce complex baseband samples. This matched filter is the square root of the Nyquist filter. Since the signals are band limited at this stage, we can decimate them by a factor of four. This is accomplished using the *demux* star. Therefore, the sampling rate is reduced from 9600 Hz to 2400 Hz. As we notice from the above galaxy, we have applied an eye diagram probe between the Nyquist filter and the *demux* star in order to observe the eye pattern of the signal before equalization. The eye diagram of the signal after echo cancellation is shown in Fig. 15.

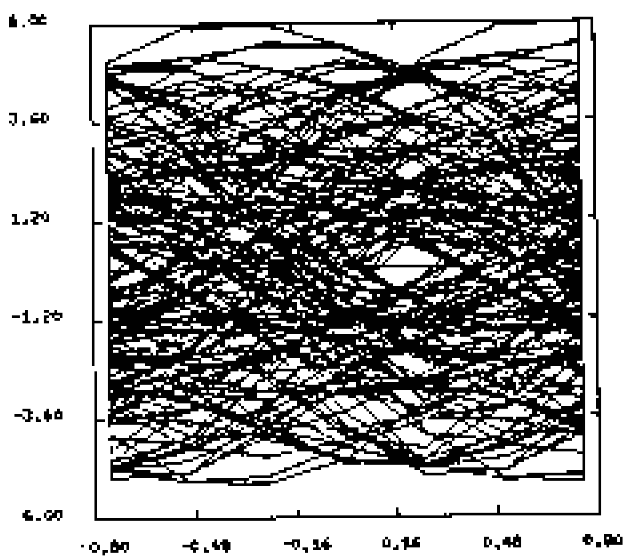

Figure 15. Eye diagram after echo cancellation (baud intervals)

We also applied a scatter star after demodulation in order to observe the signal constellation before entering the equalizer galaxy. Fig. 16 shows the signal constellation without equalization.

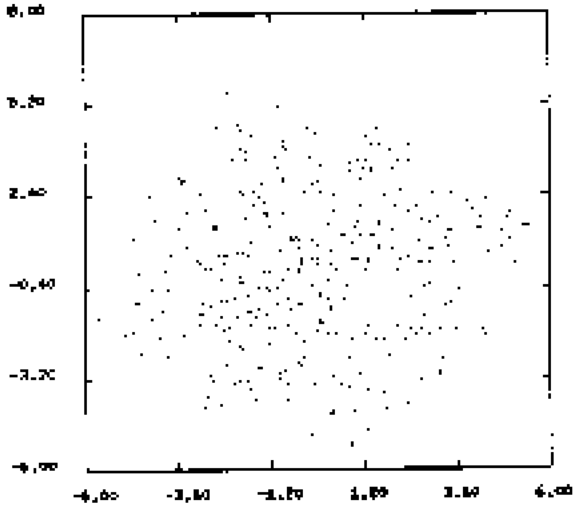

Figure 16. Signal constellation without equalizer

It is clear from the plot that the signals are widely scattered on the plot due to Inter-Symbol Interference (ISI) caused by the passband channel and in particular the phase distortion of the IIR filter in the telephone circuit galaxy. This problem will be solved when we introduce the adaptive equalizer.

3.4.3 Adaptive Equalization

Fig. 17 illustrates the topology of the adaptive equalizer. The input terminals(2&3) receive the data from the output of the scatter star (Fig. 12). The scatter star bypasses the incoming signals through the star without any changes.

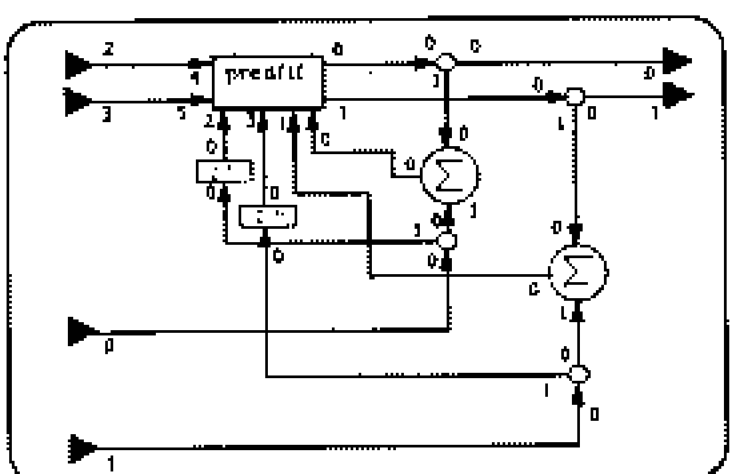

Figure 17. Block diagram of the adaptive equalizer

We have implemented a multi-channel fractionally spaced adaptive equalizer with decision feedback using the fast RLS adaptive filtering algorithm [32]. Input terminals(0&1) in Fig. 16, are the training sequence of the adaptive equalizer, and output terminals(0&1) carry the equalized baseband complex signals. The decisions are made in the decision galaxy called decisionv29 which is shown in Fig. 18.

The output terminals(0&1) are the decision feedback samples for the adaptive equalizer. The decisions are toggled between the slicers and the training symbols. The training signal are shown coming from the outputs of the remote transmitter, Fig. 3. These are normally provided by the receiver. They are input from the input terminals(0&1) in the

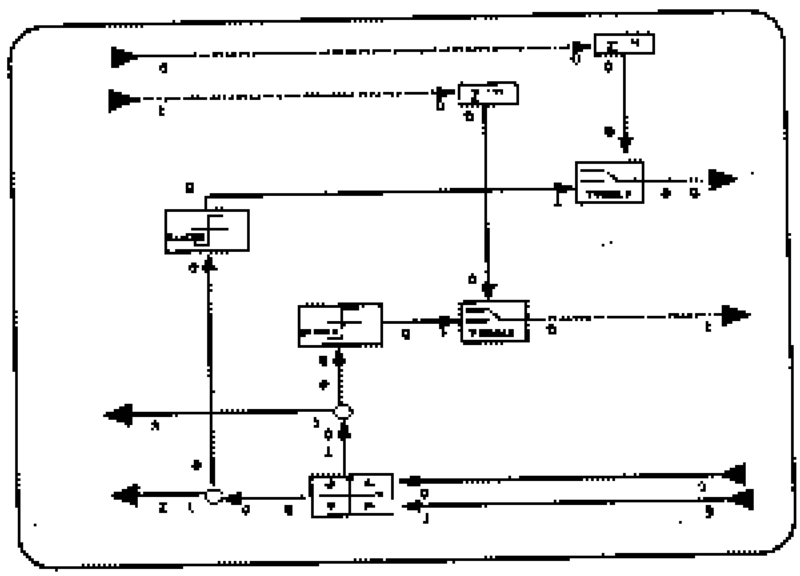

Figure 18. Block diagram of the decisionv29 galaxy

above diagram. A *delay* star is applied in this galaxy in order to compensate the delay of signals coming from the remote transmitter to the local receiver. This delay value is proportional to the number of taps used in both the adaptive echo canceller and the equalizer. In our case, we applied a 19 symbols delay in the delay star in order for the equalizer to make the correct decisions. In this simulation, while the echo canceller is adapting, the equalizer is turned off. Therefore, we have applied a 200 samples wait for the equalizer in order for the echo canceller to finish adapting to the echo path. We have also applied a scatter star after equalization in order to observe the signal constellation after equalization. Fig. 19 illustrates the performance of the equalizer.

We must note that the equilizer using the LMS algorithm could not converge with realistic telephone channels. Only for simple low pass channels did the LMS algorithm

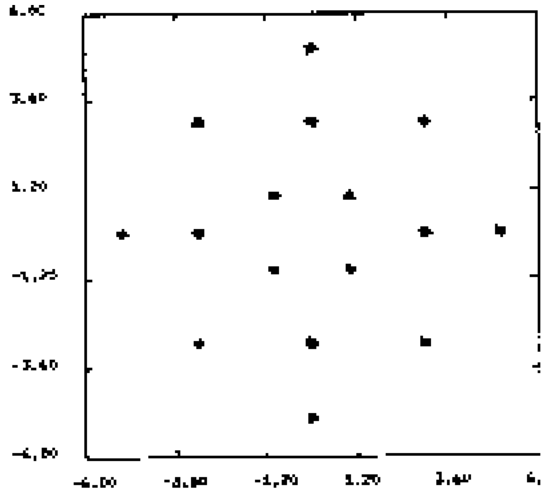

Figure 19. Signal constellation after equalization

converge. The reason for this is in the formulation of the LMS adaptive filter. This algorithm does not effectively use all of the information in its input channels to estimate the desired response. The general order multi-channel algorithm on the other hand is derived from a vector space formulation and no approximations are made. See reference [30].

3.4.4 v29 Decoder

The last galaxy of the local-receive galaxy is the V.29 decoder. This galaxy receives the coordinates of the signal constellation coming out of the *decisionv29* galaxy and applies the minimum distance detection technique in order to decode the incoming signal. Fig. 20 illustrated the decode galaxy.

As we have mentioned previously, output terminal(3) of the remote-transmit galaxy outputs the same bit pattern generated by the *bdata* star to the input terminal(0) of the decode galaxy for error counting. This means that, by using the *ecount* star we can compare the decoded output with the original bits generated by the random generator. After running the simulation, the error counter types the bit error rate (BER) on the computer screen. This value was equal to 1.4×10^{-5}.

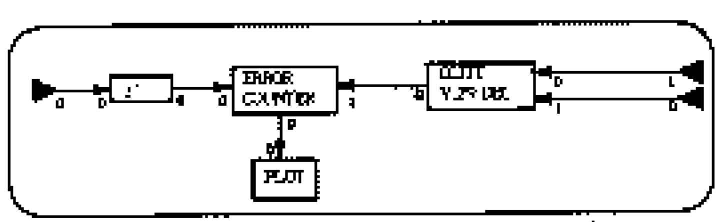

Figure 20. Block diagram of the decode galaxy

4. Performance Comparison between the LMS and the RLS Algorithms

4.1. Double Precision Implementation

The last part of this section is the comparison of the two adaptive filtering algorithms in echo cancellation. These two algorithms, as mentioned previously, are the fast RLS algorithm (FTF), and the LMS algorithm. Referring to the Fig. 13, we have substituted the *predftf* star with the *predlms* star in order to compare the performance of the two adaptive filtering algorithms. In both cases, we have set the echo canceller to adapt for 200 samples. As was mentioned previously, while the echo canceller is adapting, the remote transmitter is off. Therefore, for the first 200 samples, the remote transmitter is not sending any information. We obtained the plot of the first 300 samples in order to compare the convergence time and also the performance of the two adaptive filtering algorithms. Fig. 21 illustrates the convergence time of the echo canceller using the LMS algorithm.

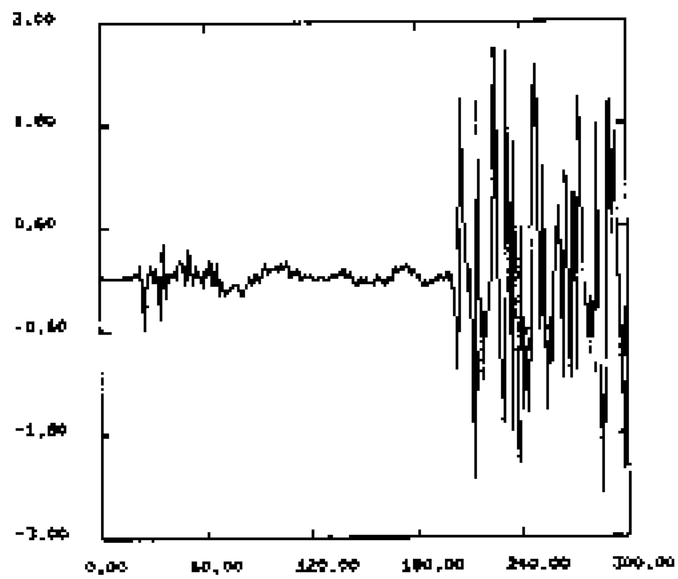

Figure 21. Convergence time of the LMS algorithm using predftf star (samples)

The first 200 samples of this plot illustrates the convergence time of the LMS algorithm. We mentioned earlier that the non-linearity of the channel caused by the non-uniform quantizer could cause problems for the echo canceller. This excess noise is very evident for the LMS algorithm; on the other hand, the RLS algorithm has much less excess noise. Fig. 22 illustrates the convergence time and the performance of the RLS adaptive filtering algorithm.

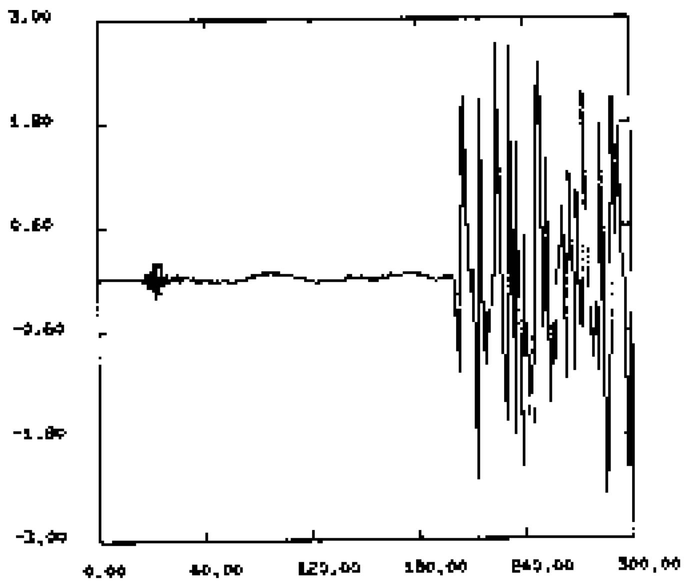

Figure 22. Convergence time of the RLS algorithm using predltf(samples)

By comparing the Fig. 21 and 22, we notice that the convergence time of the RLS algorithm is much faster than the LMS algorithm. In fact it is on the order of the number of taps of the echo canceller. Also, the excess noise due to the echo canceller is larger for the LMS algorithm. Fig. 23 shows the grouped plot of the Fig. 21 and 22. The dashed curve is the LMS algorithm.

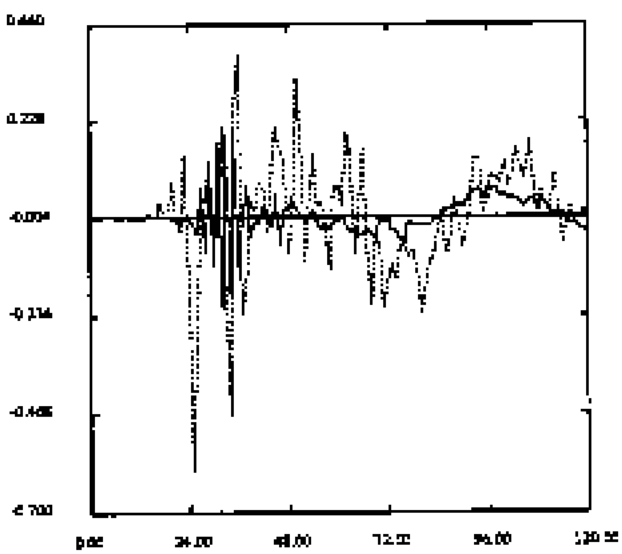

Figure 23. Group plot of the convergence time

Better performance can be achieved afterwe replaced the *predftf* star which implements the 7N FTF algorithm, by the order 10N *dbl_ftf* star. This algorithm requires a greater number of computations but has better stability. This 10N version of the FTF algorithm uses error feedback techniques [20] to improve numerical stability. The prediction error using this new star, *dbl_ftf*, is shown in Fig. 24. By adjusting the initialization parameter in dbl_ftf we are able to get very low excess error.

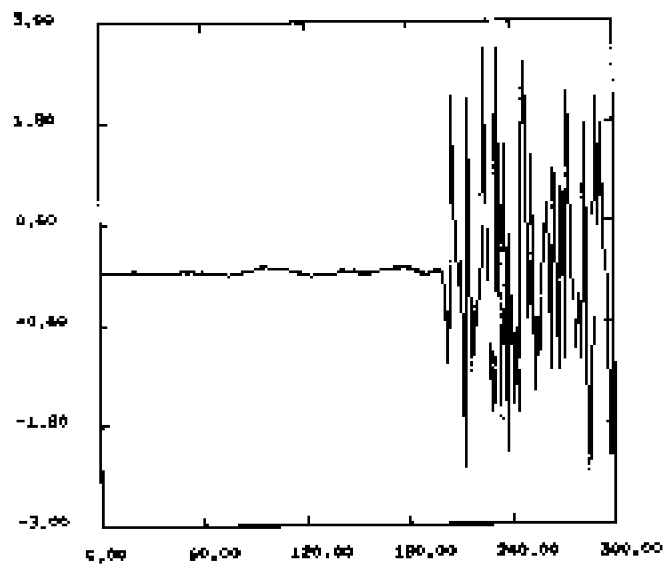

Figure 24. Convergence time of the RLS algorithm using dbl_ftf star (samples)

For μ-law companding the quantization noise increases as the input level increases; but the signal to noise ratio remains constant. In adaptive filtering, it is normally assumed that the noise is stationary and white. However, in this case the noise variance changes with the desired response level due to companding. For the echo canceller, we observe in Fig. 24 that the echo residual has a wavy shape. This shape actually follows the envelope of the echo signal which is due to the fact that the quantization level is changing. These non-linear effects can severely degrade the performance of adaptive filters and thus overall system performance.

Previously, in Fig. 19, we illustrated the signal constellation of the system using the RLS algorithm for the echo canceller. In Fig. 25, we illustrate the signal constellation of the system using the LMS adaptive filtering algorithm for echo cancellation. It is obvious that the constellation of the Fig. 19 is clearer than the one in Fig. 25 which means the excess error for the RLS algorithm is lower than the LMS algorithm.

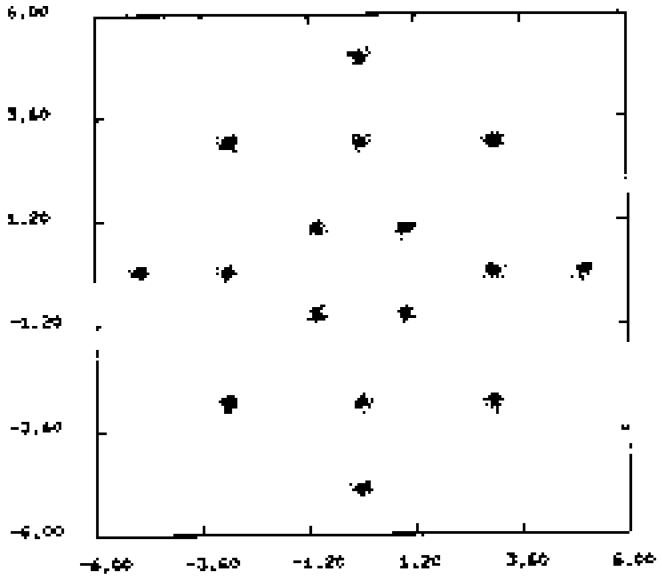

Figure 25. Signal constellation using the LMS echo canceller

4.2. Fixed Point Implementation

To study the effects of using finite-precision on the performance of the algorithms, we have implemented the fixed point versions of the FTF and the LMS algorithms. It uses different order of computations: 7N, 8N and 9N to improve numerical stability [20]. Both algorithms use 16 bit registers with 32 bit accumulation.

We have in Figures 26 and 27 the convergence characteristics of the two algorithms where we have used 8 bits for representing the fractional part of the algorithmic quantities and for the quantization of the data. Comparing the two figures with the previous ones, Figures 21 and 22, where double precision was used, it is clear that using finite precision enhances the excess error. But again the effect of using finite precision manifests itself more in the case of the LMS algorithm. Using the fixed point LMS star for echo cancellation resulted in a lower SNR at detection than the fixed point FTF star, and the bit error rate was higher for the LMS. This can also be seen by comparing the signal constellations of the two algorithms in Figures 28 and 29. Using the fixed point LMS star for echo cancellation resulted in a lower SNR at detection than the fixed point FTF star, and the bit error rate was higher for the LMS. This can also be seen by comparing the signal constellations of the two algorithms in Figures 28 and 29. We decreased the number of bits used for the fractions in the fixed point FTF to 7 and then to 6 bits. This prevented the overflow, and is a less expensive implementation. But the SNR ratio at detection decreased and the bit error rate increased because of the larger quantization errors. This clearly indicates a trade-off in the choice of the register lengths and the number of bits for fraction. The signal constellation for the fixed point FTF with 6 bits for the fraction is given in Fig. 30 .

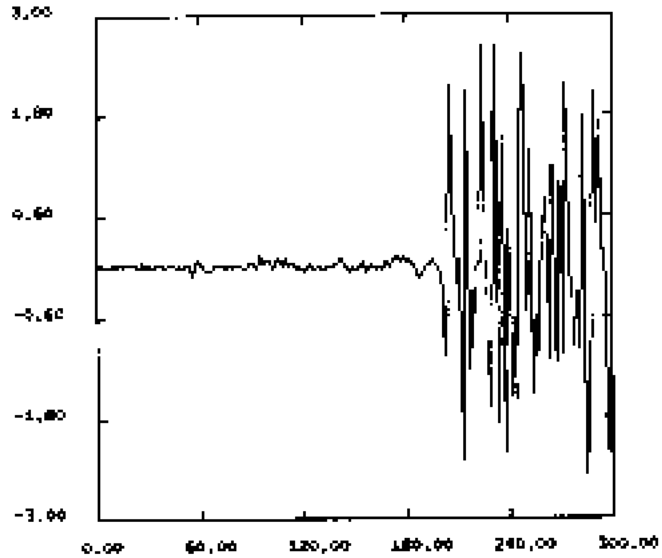

Figure 26. Convergence time using fixed point FTF for the echo cancellation, 8 bits fraction (samples)

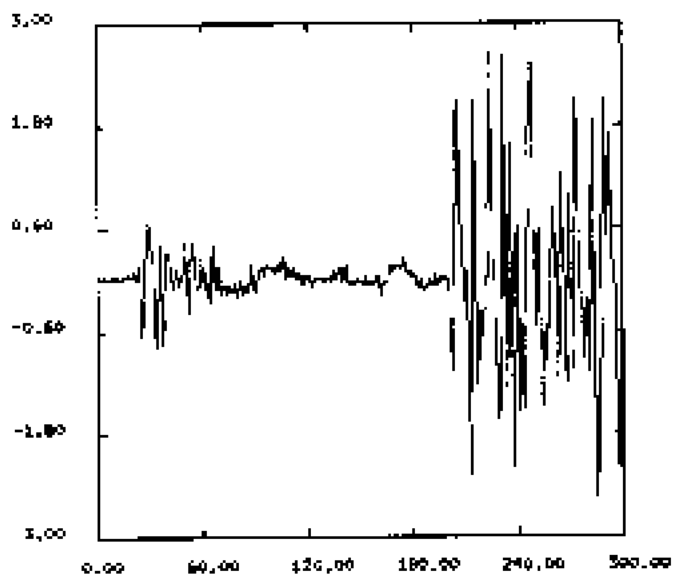

Figure 27. Convergence time using fixed point LMS for the echo cancellation, 8 bits fraction (samples)

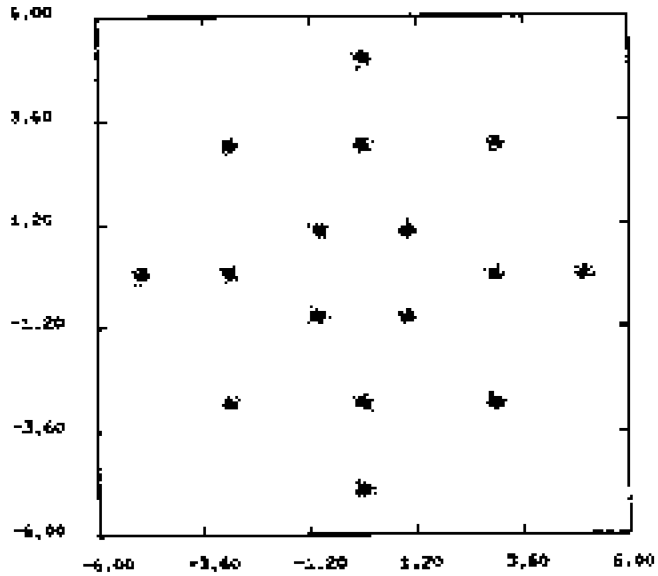

Figure 28 Signal constellation using fixed point FTF for echo cancellation, 8 bits fraction

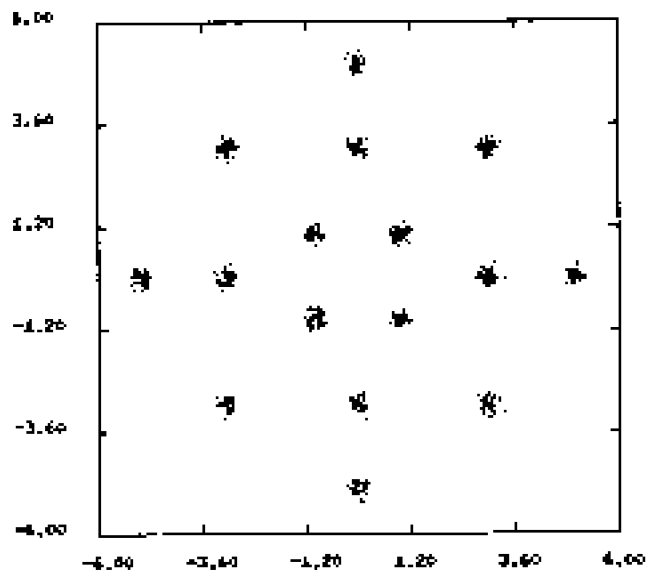

Figure 29. Signal constellation using fixed point LMS for echo cancellation, 8 bits fraction

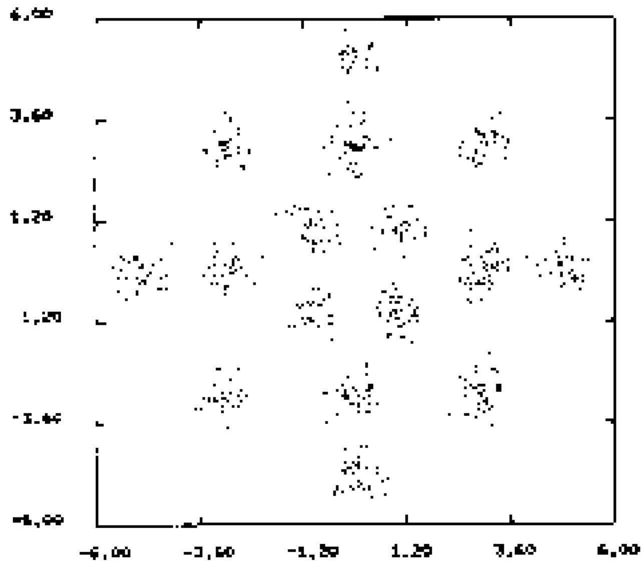

Figure 30. Signal constellation using fixed point FTF, 6 bits for fraction

5. Conclusion

The performance of the FTF algorithm is evaluated using a detailed block diagram simulation of a full-duplex 9600 bps voiceband modem. All major components of the system were modelled and simulated including accurate models for realistic channels (μ-law quantization noise and amplitude and phase distortion). In this application, the adaptive filter is used both for adaptive complex decision feedback equalization and echo cancellation. The performance of the FTF algorithm is compared with the conventional normalized LMS algorithm for both the floating point and the fixed point implementations. It is found that while the LMS algorithm failed to perform in typical and worst case channels, the multi-channel general order FTF algorithm performed flawlessly and effectively removed channel distortion and interference.

6. REFERENCES

[1] L. Ljung and T. Soderstrom, *Theory and Practice of Recursive Identification*, MIT Press, 1983.

[2] John M. Cioffi and A Thomas Kailath, "Fast, recursive-least-squares transversal filters for adaptive filtering" *IEEE Transactions on Acoustics, Speech, and Signal Processing*, Vol ASSP-32, No. 2, April 1984, pp. 304-337.

[3] G. Carayannis, D.G. Manolakis, N. Kalouptsids,"A fast sequential algorithm for least-squares filtering and prediction,"*IEEE Transactions on Acoustics, Speech, and Signal Processing*, Vol ASSP-32, No. 2, April 1984, pp. 304-337.

[4] Sasan H. Ardalan, Jim Faber, "Derivation of the Fast Pole-Zero (ARMA) Recursive Least Squares Algorithm Using Geometric Projections" *IEEE Trans. on Acoustics, Speech and Signal Processing*, pp. 349-358, March 1986.

[5] L. J. Faber, S. H. Ardalan, S.T. Alexander, "A Derivation of a General Order, Multichannel, Fast Transversal, Recursive Least Squares Filter Algorithm," *1986 IEEE Military Communications Conference*, Monterey, CA, October 5-9, 1986.

[6] D.D. Falconer and L. Ljung, "Application of Fast-Kalman estimation to adaptive equalization," *IEEE Transactions on Communication*, Vol. COMM-26, No. 110, Oct. 1978.

[7] S. Ljung and L. Ljung, "Error propagation properties of recursive least-squares adaptation algorithms,"*Automatica*, Vol. 21, No. 2, March 1985.

[8] M. Bellanger and C. C. Evci, "Coefficient wordlength limitation in FLS adaptive filters," *Proceedings of ICASSP 86*, April 7, 1986, Tokyo, Japan, pp 3011-3014.

[9] J. Botto, "Stabilization of fast Recursive Least Squares transversal filters for adaptive filtering." *Proc. IEEE ICASSP* 87, Dallas, Texas, pp. 403-407.

[10] Sasan Ardalan, S.T. Alexander, "Fixed point roundoff error analysis of the exponentially windowed RLS algorithm for time-varying systems," *IEEE Trans. on Acoustics Speech and Sig. Proc.*,Vol. ASSP-35, No. 6, June 1987.

[11] Sasan H. Ardalan,"Floating point roundoff error analysis of the RLS and LMS adaptive algorithms,"*IEEE Trans. on Circuits and Systems*, Vol. CAS-33, No. 12, December 1986, pp. 1192-1208.

[12] John M. Cioffi, "Limited precision effects in adaptive filtering", *IEEE Trans. on Circuits and Systems*, Vol. CAS-34, No. 7, July 1987.

[13] Christos Caraiscos, Bede Liu, "A roundoff error analysis of the LMS adaptive algorithm," *IEEE Trans. on Acoustics, Speech and Signal Processing*, Vol. ASSP-32, No. 1, February 1984.

[14] R.D. Gitlin et al, "On the design of gradient algorithms for digitally implemented adaptive filters, "*IEEE Trans. on Circuit Theory*, vol. CT-20, pp. 125-136, March 1973.

[15] Sasan Ardalan, "On the sensitivity of RLS algorithms to perturbations in the filter coefficients," *IEEE Trans. on Acoustics, Speech and Signal Processing*, November 1988.

[16] John M. Cioffi, "When do I use an RLS adaptive filter?," *Asilomar Conference on Communication, Control and Computers*, Monterey, CA, November 1986.

[17] N. J. Bershad, "Dynamic range and finite word effects in digital implementation of the LMS algorithm," *Int. Symposium on Circuits and Systems*, June 1988.

[18] Maurice G. Bellanger, "Computational complexity and accuracy issues in fast least squares algorithms for adaptive filtering," *Int. Symposium on Circuits and Systems*, June 1988.

[19] J. M. Cioffi, "Precision-efficient use of block adaptive algorithms in data-driven echo cancellers," *Int. Conference on Communications (ICC88)*, June 1988.

[20] D.T.M. Slock and T. Kailath, "Numerically stable fast recursive least-squares transversal filters," *Int. Conf. on Acoustics, Speech and Sig. Proc. (ICASSP88)*, April 1988.

[21] Sasan Ardalan, "Finite wordlength analysis of the LMS adaptive filter algorithm," CCSP Technical Report, CCSP-TR-84/4, Dept. of Elect. and Comp. Eng., NC State University, February 1984.

[22] Tulay Adali, Sasan Ardalan, " Roundoff Error Analysis of RLS Algorithms With Correlation," *International Conference on Acoustics Speech and Signal Processing (ICASSP)*, New Mexico, April 1989.

[23] Tulay Adali, Sasan Ardalan, "Transient Analysis of Finite Precision RLS Adaptive Filters" *International Symposium on Circuits and Systems*. New Orleans, Louisiana, May 1990.

[24] Ramin Nobakht, Sasan Ardalan, D. E. Van den Bout, "Nonlinear Adaptive Filtering and Mean Field Annealing," *International Symposium on Circuits and Systems*, New Orleans, Louisiana, May 1990.

[25] Sasan Ardalan, "CAD of Digital Communications Systems with Complex Transmission Line Networks," *National Communications Forum*, Chicago, Ill., Sept. 28-30, 1987 (Invited).

[26] Russell Barnes, Sasan Ardalan, "Design and Implementation of a Multiprocessor Architecture for Adaptive Digital Filtering," *International Conference on Communications*, Toronto, Canada, June 1986.

[27] T. K. Miller, S. H. Ardalan, "A Multiprocessor Configuration for the Adaptive Fast Kalman Algorithm," *International Conference on Communications*, Toronto, Canada, June 1986.

[28] Recommendation V.29,"9600 bits per second modem standardized for use on point-to-point 4-wire leased telephone-type circuits," *CCITT(International Telegraph and Telephone Consultive Committee)*, Red book, vol.III, 1984.

[29] Hui-Hung Lu, David Hedberg, and Bernard Fraenkel, "Implementation of high-speed voiceband data modems using the TMS320C25," *ICASSP 1987*, pp 1915-1918.

[30] Oscar Agazzi, David G. Messerschmitt, and David A.Hodges, "Nonlinear echo cancellation of data signals," *IEEE Trans. on Communications*, vol.com-30, No.11,pp 2421-2422, November 1982.

[31] Mark J.Smith, Colin F.N. Cowan, and Peter F.Adams,"Nonlinear echo cancellers based on transpose distributed arithmetic, "IEEE *Trans. on Circuits and Systems*,vol.35, p. 6, January 1988.

[32] L.J Faber, "A general order multichannel, fast least squares algorithm with telecommunications applications," Ph.D. thesis, NCSU,1988.

[33] Shahid Qureshi, "Adaptive Equalization", Proceedings of the IEEE, Vol. 73, No. 9, September 1985.

[34] T. A. C. M. Claasen, W. F. G. Mecklenbrauker, "Adaptive Techniques for Signal Processing in Communications," IEEE Communications Magazine, November 1985.

[35] Kaveh Pahlavan, Jerry L. Holsinger, "Voice-Band data communication modems - a historical review: 1919-1988," *IEEE Communication Magazine*, Vol. 26, No. 1.